Towards successful cleaning of chert samples for improved 10Be and 26Al measurements

Regis Braucher, Hidy Alan J., Matmon Ari, D.L. Bourles, Georges Aumaitre, Keddadouche Karim

Towards successful cleaning of chert samples for improved ^{10}Be and ^{26}Al measurements

Braucher Régis[1,*] ; Hidy Alan J.[2,3], Matmon Ari[3] ; Bourlès Didier[1]; Aumaître Georges[1]; Keddadouche Karim[1] .

1: CEREGE, Aix-Marseille Univ., CNRS, IRD, Coll. France, INRA, UM 34

2: Center for Accelerator Mass Spectrometry, Lawrence Livermore National Laboratory, Livermore, CA 94550, USA

3: The Fredy & Nadine Herrmann Institute of Earth Sciences, The Hebrew University of Jerusalem, Edmond J. Safra Campus, Jerusalem 91904, Israel

*: corresponding author; Email: braucher@cerege.fr

Abstract

In situ-produced cosmogenic ^{10}Be and ^{26}Al measurements are widely applied in geomorphological studies and in archaeology and paleoanthropology as a chronologic tool applicable to the past 5 Ma. While most of these measurements are made from concentrates of quartz, a ubiquitous and resistant mineral, it is of great interest to extend this method to other silicates and particularly to the amorphous silicates whose purification may not be as straightforward. This paper presents a cleaning procedure that has been applied on ten samples of various siliceous rocks (chert, granite and quartzolite). The aim is to monitor the ^{10}Be, ^{27}Al and ^{26}Al concentration evolution as a function of cleaning steps. While this protocol appears suitable for ^{10}Be, when measuring ^{26}Al careful attention should be paid to ^{27}Al, whose concentration should be measured regularly to ensure that a constant value is achieved and most important, allowing measuring ^{26}Al/^{27}Al by AMS.

Keywords: Beryllium, Aluminum, Cosmogenic, Silicate, ASTER.

Introduction

Measurements of in situ-produced ^{10}Be and ^{26}Al are routinely used for determining exposure or burial durations and denudation rates. In quartz, these cosmogenic nuclides are mainly produced through spallation reactions on oxygen and silicon. Quartz is presently the mineral of choice because it is ubiquitous, resistant to alteration, and a means of purification is established. Thus, huge efforts have been made to calibrate ^{10}Be and ^{26}Al production rates within this mineral (e.g. Nishiizumi et al., 1989, Evans et al., 1997, Balco et al, 2009, Putnam et al. 2010, Kaplan et al, 2011, Borchers 2016). However, for other silicate minerals (feldspars, sanidine, chert), obtaining pure mineral fractions is not as straightforward and requires more attention (Zerathe et al. (2013, 2017); Kober et al. (2005)).

^{10}Be and ^{26}Al concentrations are calculated from measurements of ^{10}Be/^{9}Be and ^{26}Al/^{27}Al by accelerator mass spectrometry (AMS). Therefore, concentrations of the stable isotope (^{9}Be or

^{27}Al), must be accurately and precisely determined before sample dissolution. Beryllium is generally negligible in most silicate minerals and thus the addition of a ^{9}Be carrier is required. Conversely, aluminum is relatively abundant in most silicate minerals, with ^{27}Al concentrations often sufficient for AMS measurement without addition of a carrier. Therefore, measurements of ^{26}Al require the natural ^{27}Al concentration to be accurately determined. In many laboratories (Mifsud et al., 2013; Corbett et al., 2016), the cleaning procedure ends when this natural content, measured on small aliquot (1-2 g) is below 100 ppm Al. These previous approaches have been shown to be suitable for well crystallized silica with homogeneous aluminum content. However, for amorphous silica with a potential heterogeneous chemical composition, this procedure may be inappropriate and could result in ^{26}Al and/or ^{10}Be concentrations that either do not solely reflect in-situ production or reflect in-situ production from uncharacterized mineral impurities (Boaretto et al 2000, Matmon et al., 2003; Guralnik et al., 2010, Zerathe et al. 2013) as evidenced by the assumed "clean" material having anomalously high ^{27}Al concentrations.

In this paper, ten samples of various siliceous rocks (chert, granite, vein quartz and quartzolite (silicified carbonate rock)) were processed and measured for ^{10}Be and ^{26}Al analyses with an adapted chemical protocol based on Zerathe et al. (2013). The purpose of this study is to 1) determine if cosmogenic ^{10}Be and ^{26}Al concentrations measured from samples of different lithologies, but collected from the same location with presumably identical exposure histories, yield identical values; and if not, 2) determine the effectiveness of additional cleaning steps at resolving any lithologic concentration differences. To do this, we monitor the ^{10}Be, ^{27}Al and ^{26}Al concentration evolutions as a function of cleaning steps. Additionally, we measure in-situ produced ^{36}Cl in carbonate-rich samples at one site (ZEB) for an independent exposure age comparison.

Samples (Braucher.kmz here)

Samples were collected in the Negev Desert, southern Israel, are from four locations named ZEB, YEH, HEM, and ARAD (refer to kmz and table 1). These locations were chosen for this experiment because each site featured geomorphic surfaces with long surface exposure histories and provided multiple silica-bearing lithologies (ZEB, HEM, and ARAD were collected from desert pavements, and YEH from eroding bedrock). From each location, samples of different lithology were collected. Considering their short identifications (Short ID, Table 1), samples 1 and 2 are from the ZEB location (chert and quartzolite respectively), samples 3, 4, and 5 are from the YEH location (chert, granite and quartz vein respectively), samples 6 and 7 are from the ARAD location (chert and quartzolite respectively) and samples 8, 9 and 10 are from the HEM location (quartzolites and two distinct types of chert, respectively). For more information on the regional geological context of these samples, one can refer to Matmon et al (2017).

With the exception of the carbonate-rich ZEB samples, all samples were crushed, decarbonated, and processed at CEREGE. These steps were not performed on the ZEB samples because it was possible to measure ^{36}Cl from the carbonate fraction as well as ^{10}Be and ^{26}Al from the chert fraction (Figure 1).

Chemical preparation and cleaning strategy for silica samples

Original samples were crushed and sieved (0.25–.85 mm), then divided into four sub-samples (Bulk; HF; KOH and KOH-*bis*) (Table 2) which were subjected to different cleaning steps. Following each cleaning step, sample concentrates were rinsed several times in ultra-pure water and dried for 24 hours at 90°C.

The Bulk sub-sample underwent no cleaning steps.

The three other sub-samples were subjected to Aqua Regia to remove the carbonate fraction and purified by selective dissolutions with HCl and H_2SiF_6. To eliminate the potential atmospheric ^{10}Be adsorbed to grain surfaces, the remaining dried and weighted samples were cleaned using sequential 48% HF dissolutions (Brown et al., 1991; Kohl and Nishiizumi, 1992; Cerling and Craig, 1994), with each step dissolving ~10% of the material.

Sub-sample HF was dissolved and processed without further cleaning.

Sub-samples KOH and KOH-*bis* were subjected to one and two rounds, respectively, of a 48 hours leaching in 3N KOH at 80°C prior to spiking and complete dissolution. As shown in Verstraete (2005) and tested in Zerathe et al (2013), the 3N KOH solution gently dissolves amorphous silica, enabling a smooth cleaning of the material and, allowing, if they are present the accumulation of micro-crystallized quartz spherules (see Zerathe et al (2013)).

Samples were dried to quantify sample loss between cleaning steps and enable the calculation of efficiency cleaning by:

Reagent efficiency = (Mass dissolved by reagent) / (Total reagent volume). This efficiency unit is in (g sample) / (ml reagent).

After cleaning, all samples were spiked with ~0.1 g of an in-house ^{9}Be carrier (3025±9 ppm; Merchel et al, 2008), totally dissolved in an acid cocktail (concentrated HF, 10 mL HNO_3, and 3 mL $HClO_4$), and then re-dissolved in 7N HCl. Final solutions were weighed and a 100µl aliquot was collected and diluted in HNO_3 2% in order to determine the ^{27}Al concentration by ICP-OES on a 6500 ICAP from Thermo Scientific.

Finally, ^{10}Be and ^{26}Al were extracted by ion exchange resins (200 mesh DOWEX® 1X8 and 50WX8), precipitated as hydroxides and converted to oxides by ignition at 700°C.

Beryllium oxide was mixed with 325 mesh niobium powder and aluminum oxide with silver powder prior to AMS measurements, which were carried out at ASTER, the 5 MV French AMS national facility at CEREGE (Arnold et al., 2010).

The ^{10}Be data were calibrated directly against STD11 in house standard ($^{10}Be/^{9}Be$ value of $(1.191\pm0.013) \times 10^{-11}$, Braucher et al. 2015). Analytical uncertainties (reported as 1σ) include uncertainties associated with AMS counting statistics, chemical blank measurements and AMS internal error (0.5%).

The measured $^{26}Al/^{27}Al$ ratios were calibrated against the ASTER in-house standard SM-Al-11 whose nominal value is $^{26}Al/^{27}Al = (7.401 \pm 0.064) \times 10^{-12}$ (Merchel and Bremser, 2004). $^{10}Be/^{9}Be$ blank ratio was 3.38×10^{-16} (± 37%), and $^{26}Al/^{27}Al$ blank ratio was 5.26×10^{-15} (±26 %).

Chemical preparation for ^{36}Cl measurements

The crushed samples (0.250- 1 mm fraction) experienced a 4h water-leaching, followed by a 10%-dissolution using HNO_3 (2 mol.l^{-1}). The resulting material was totally dissolved in HNO_3 after addition of ~1.5 mg of a ^{35}Cl-enriched carrier ($^{35}Cl/^{37}Cl$ ~ 800) allowing natural chlorine determination by isotope AMS dilution. Potential residues were recovered from the solution for further ^{10}Be and ^{26}Al preparations. After taking an aliquot for Ca-determination by ICP-OES, 1 ml of an $AgNO_3$ solution (10%) was added to the dissolved sample to precipitate AgCl. To reduce ^{36}S isobaric interference during AMS measurement of ^{36}Cl, the AgCl precipitate was re-dissolved using NH_4OH, and sulfur was co-precipitated with $BaCO_3$ as $BaSO_4$ by addition of a slightly ammoniac saturated $Ba(NO_3)_2$ solution. The final AgCl-target was produced by re-precipitation using HNO_3, repeated washing cycles with HNO_3 and H_2O and drying at 80°C. Chlorine AMS measurements were performed at the ASTER AMS national facility (CEREGE, Aix en Provence, France) (Klein et al, 2008; Finkel et al., 2013), and normalized using KNSTD1600 calibration material ($^{36}Cl/^{35}Cl=2.112 \times 10^{-12}$) (Sharma et al, 1990).

Results and discussion

^{36}Cl measurements

The ^{36}Cl, natural ^{35}Cl and Ca concentrations of carbonate fractions of samples 1 and 2 are presented in sub table 3. As the ^{35}Cl concentrations are low, no extra isotopic determination were performed on these samples. Long term denudation rates or minimum exposure durations have been determined using a mean production rate of (42.2 ±2) at/g/yr (Schimmelpfennig et al 2009; Braucher et al. 2011) and the muon scheme of Braucher et al. (2011). These denudation rates and exposure ages are 2.19 ± 0.07 m/Ma and 275 ± 9. ka for sample1 and 0.18 ± 0.01 m/Ma and 1065 ± 37ka for sample 2. These denudation rates and exposure durations are in agreement with previous measurements from the same location (Matmon et al., 2016).

^{10}Be concentrations:

The ^{10}Be concentrations behave as expected. They indeed decrease as the number of cleaning steps increases until a plateau corresponding to the sole in situ-produced ^{10}Be concentration is reached, (Brown 1991). Thus at this stage, one can say that the proposed cleaning procedure (3HF cleaning steps plus 2 cleanings in 3N KOH) allows obtaining accurate in situ-produced ^{10}Be concentrations for chert (Figure 2 and Table 3).

^{27}Al concentrations:

As for ^{10}Be, ^{27}Al concentration evolutions were determined all along the cleaning process. It is thus possible to monitor the cleaning efficiency of each individual step (Table 4).

Samples 5 (quartz) and 7, 8, (quartzolites) yield the lower efficiencies for both HF and KOH, between 0.28 and 0.32 g/ml for HF and below 0.06 g/ml for KOH. The HF efficiency corresponds to that expected from a stoichiometric reaction of HF (48%) on well crystallized SiO_2. However, there is a reduced effect of KOH on the quartzolite.

For other samples both cleaning efficiencies are higher. HF efficiency ranges from 0.38 up to 0.75g/ml and the KOH efficiency ranges from 0.075 up to 0.26 g/ml. A value higher than 0.32g/ml for HF and higher than 0.075 g/ml for subsequent KOH leachings appears to be related to poorly-crystallized or amorphous mineral phases.

Four samples (2, 3, 4 and 10) with high HF efficiencies exhibit a high release of ^{27}Al after the HF cleaning. This is unexpected since selective dissolution is typically employed to reduce the relative abundance ^{27}Al with respect to the silica concentrate, and this is in spite of the careful washing that was performed before drying the remaining sample. In fact, such high ^{27}Al content (several hundred to thousands of ppm!) would be expected in the leachate rather than the remaining silica concentrate

These unexpected ^{27}Al peaks may therefore be linked to a highly inhomogeneous distribution of the elements within the studied samples. To better understand this, it would be interesting in future to perform in situ measurements (such as X-ray fluorescence spectrometry) to localize if they exist, potential ^{27}Al enriched phases or potential sites that may have the ability do complex cations. Sample 4, described as granite presents a dual behavior with a high efficiency for the 3 HF leachings as observed for chert samples but a low efficiency with KOH solution as observed for pure quartz or quartzite. This sample also exhibit unexpected high ^{27}Al content.

To conclude, it appears important to monitor the ^{27}Al content after each cleaning step (Figure 3). If a plateau is reached, as for samples 3, 7, 8 and probably 9, the material is ready for total dissolution and for ^{26}Al measurement. However, the magnitude of the plateau in ^{27}Al concentration should also be considered. If it is of the order of several hundred of ppm Al, then it might result in a $^{26}Al/^{27}Al$ too low to be measured by AMS.

^{26}Al concentration.

Among the 38 prepared samples, no ^{26}Al was detected in two of them (4-HF and 4-KOH), only one event was counted (100% uncertainty) for two others (4-Bulk and 4-KOH-*bis*) and 10 of them did not reach the minimum $^{27}Al^-$ current (20 nA at the high energy faraday cup) for an accurate AMS measurement. For the remaining samples, the mean $^{27}Al^-$ currents were between 300 and 20 nA. Based on these data, it seems that the chemical composition of the mineral may be the reason of such poor currents. This was also the case in a previous attempt to measure samples 13-IL-ZEB-02C and 13-IL-HEM-17 at LLNL where low currents were also obtained.

Denudation rates and minimum exposure durations.

The main purpose of this paper was to develop a chemical procedure enabling to measure in situ-produced cosmogenic nuclides (^{10}Be and ^{26}Al) within silica samples of various compositions. Although the results concerning aluminum must imperatively be improved, it is important to present the output of these measurements (mainly ^{10}Be concentrations) in term of geomorphological information such as denudation rates or minimum exposure durations (Table 5).

Basically, denudation rates were determined assuming steady state and minimum exposure ages were calculated assuming no denudation. Production parameters have been scaled using Stone polynomial (Stone 2000 after Lal 1991) and a standard atmosphere. The spallation sea level production rate is the one presented by Borchers et al. (2016) that is (4.02 ± 0.18) at/g/a and the muon contributions from Braucher et al. (2011).

As the bulk fractions were not clean, their results will not be discussed.

Denudation rate and minimum exposure duration have been determined for the ZEB location from ^{10}Be and ^{36}Cl concentrations. Both nuclides yield to similar results. Sample 1 yields exposure ages of 256 ± 25 ka and 275 ± 9 ka for ^{10}Be and ^{36}Cl respectively in total agreement with the ages of 241±26 ka and 248±27ka determined by Matmon et al.(2016) using ^{10}Be only.

Considering sample 2, despite a constant ^{10}Be concentration on the order of 7.5 ± 0.2 Mat/g it seems that this sample is saturated. For this sample, Matmon et al. deduced exposure ages of 1671 ± 267 ka and 1950 ± 338 ka for the coarse and fine fractions from ^{10}Be measurements. For ^{36}Cl the carbonate fraction allows determining an age of 1065 ± 37 ka.

For the YEH samples, the chert sample number 3 appears to be more resistant to denudation than the neighboring granite (Sample 4) or quartz vein (sample 5). This surface experienced denudation rates ranging from 7 to 17 m/Ma and is exposed at least since 40 ka.

For the ARAD samples composed of a chert (sample 6) and a quartzite (sample 7), the outputs of both samples are comparable and yield to a denudation rate lower than 1.5 m/Ma and a minimum exposure duration of 350 ka. Again, chert samples seem to be more resistant than the co-existing quartzite.

The last group, HEM, presents similar results for the quartzite sample 8 but a slightly lower denudation rate for the 2 others chert samples (9 and 10). Here again, chert fraction appears to be more resistant than quartzite. Based on the two chert sub samples (9 and 10), the minimum exposure duration of the surface is of the order of 1.1 Ma.

Conclusions

In this paper, a cleaning procedure derived from that used for quartz mineral, but adapted for other silica minerals, is presented. The main outputs are:

- It is important to monitor the leaching efficiency throughout the cleaning procedure. A value closed to 0.3 g of material dissolved per milliliter of HF indicates “well” crystallized quartz. A higher value may indicate the presence of an amorphous phase.
- In case of amorphous phase, the use of a 3N KOH solution at 80°C for 2 days may help to gently dissolve the amorphous phase. This step has to be done at least twice.
- It is important to measure ^{27}Al content after each cleaning step in KOH to ensure that a concentration plateau is reached. In this study, 2 KOH leachings were not sufficient for all samples.
- Based on ^{10}Be only, chert samples seem to be more resistant than quartz to denudation processes in desert environment.

As described in Zerathe et al (2013), thin sections of the chert samples may help to better characterize the chert structure. In some chert types, micro crystalline quartz can be present. If it is the case, the cleaning procedure described in this paper will then allow the accumulation of this micro crystalline quartz throughout all cleaning steps.

Acknowledgements

ASTER AMS national facility (CEREGE, Aix en Provence) is supported by the INSU/CNRS, the ANR through the "Projets thématiques d’excellence" program for the "Equipements d’excellence" ASTER-CEREGE action and IRD. RB thanks Laetitia Leanni and Valery Guillou for fruitful discussions. A component of this work was performed under the auspices of the U.S. Department of Energy by Lawrence Livermore National Laboratory under Contract DE-AC52-07NA27344. This is LLNL-JRNL-745527. The authors thank S. Zerathe for thoughtful suggestions that improved the manuscript.

References:

Arnold M., Merchel S., Bourles D.L., Braucher R., Benedetti L., Finkel R.C., Aumaître G., Gottdang A. & Klein M., 2010. The French accelerator mass spectrometry facility ASTER: Improved performance and developments. Nuclear Instruments and Methods in Physics Research B, 268: 1954 - 1959.

Balco, G., Briner, J., Finkel, R.C., Rayburn, J.A., Ridge, J.C., Schaefer, J.M., 2009. Regional Beryllium-10 production rate calibration for late-glacial northeastern North America. Quaternary Geochronology. 4, 93-107.

Boaretto, E., Berkovits, D., Hass, M., Hui, S.K., Kaufman, A., Paul, M., Weiner, S., 2000. Dating of prehistoric cave sediments and flints using ^{10}Be and ^{26}Al in quartz from Tabun Cave, Israel. Nuclear Instruments and Methods in Physics Research. B 172, 767 - 771.

Borchers B., Marrero S., Balco G., Caffee M., Goehring B., Lifton N., Nishiizumi K., Phillips F., Schaefer J., Stone J., 2016. Geological calibration of spallation production rates in the CRONUS-Earth project, Quaternary Geochronology, 31, 188-198

Braucher R., Guillou V., Bourlès D.L., Arnold M., Aumaître G., Keddadouche K., Nottoli E. 2015. Preparation of ASTER in-house^{10}Be/^{9}Be standard solutions. Nuclear Instruments and Methods in Physics Research B 361 335-340

Braucher, R., Merchel, S., Borgomano, J., Bourlès, D., 2011. Production of cosmogenic radionuclides at great depths: A multi element approach. Earth Planet. Sci. Lett. 309, 1-9.

Brown, E.T., Edmond, J.M., Raisbeck, G.M., Yiou, F., Kurz, M.D., Brook, E.J., 1991. Examination of surface exposure ages of antarctic moraines using insitu produced Be-10 and Al-26. Geochimica and Cosmochimica Acta 55, 2269-2283.

Cerling, T.E. and Craig, H., 1994. Geomorphology and in-situ cosmogenic isotopes. Annual Reviews of Earth and Planetary Sciences, 22: 273-317.

Corbett L. B., Bierman P. R., Rood D. H., 2016. An approach for optimizing in situ cosmogenic ^{10}Be sample preparation, Quaternary Geochronology, 33, 24-34,

Evans, J.M., Stone, J.O.H., Fifield, L.K., Cresswell, R.G., 1997. Cosmogenic chlorine-36 production in K-feldspar. Nuclear Instruments and Methods in Physics Research. B 123, 334-340

Finkel R., Arnold M., Aumaître G., Benedetti L., Bourlès D., Keddadouche K., Merchel S., Improved ^{36}Cl performance at the ASTER HVE 5 MV accelerator mass spectrometer national facility, Nuclear Instruments and Methods in Physics Research. B, 294, 121-125, (2013).

Guralnik, B., Matmon, A., Avni, Y., Fink, D., 2010. ^{10}Be exposure ages of ancient desert pavements reveal Quaternary evolution of the Dead Sea drainage basin and rift margin tilting. Earth and Planetary Science Letters. 290, 132-141.

Kaplan, M.R., Strelin, J.A., Schaeffer, J., Denton, G.H., Finkel, R., Schwartz, R., Putnam, A.E., Goehring, B.M., Travis, S.G., 2011. In-situ cosmogenic ^{10}Be production rate at Lago Argentino, Patagonia: Implications for late-glacial climate chronology. Earth and Planetary Science Letters, 309, 21-32.

Kober F., Ivy-Ochs S., Leya I., Baur H., Magna T., Wieler R., Kubik P.W., 2005, In situ cosmogenic ^{10}Be and ^{21}Ne in sanidine and in situ cosmogenic 3He in Fe–Ti-oxide minerals, Earth and Planetary Science Letters, 236, 1–2, 404-418

Kohl C.P, Nishiizumi K,1992. Chemical isolation of quartz for measurement of in-situ -produced cosmogenic nuclides, Geochimica et Cosmochimica Acta, 56, 9,3583-3587.

Klein G., Gottdang A., Mous D.J.W., Bourlès D.L., Arnold M., Hamelin B., Aumaître G., Braucher R., Merchel S., Chauvet F., 2008, Performance of the HVE 5 MV AMS system at CEREGE using an absorber foil for isobar suppression, Nuclear Instruments and Methods in Physics Research. B 266, 1828-1832.

Matmon, A., Crouvi, O., Enzel, Y., Bierman, P., Larsen, J., Porat, N., Amit, R., Caffee, M., 2003. Complex exposure histories of chert clasts in the late Pleistocene shorelines of Lake Lisan, southern Israel. Earth and Surface Processes and Landscape. 28, 493 - 506.

Lal D. 1991. Cosmic ray labeling of erosion surfaces : in-situ nuclide production rates and erosion models. Earth and Planetary Science Letters, 104, 424-439.

Matmon, A., Elfassi, S., Hidy, A., Geller, Y ., Porat, N ., ASTER Team , 2016. Controls on aggradation and incision in the NE Negev, Israel, since the middle Pleistocene. Geomorphology, v. 261, p. 132-146.

Merchel, S., Bremser, W., 2004. First international ^{26}Al interlaboratory comparison – Part I. Nuclear Instrumentation Methods in Physics Research, B: Beam Interactions with Materials and Atoms. 223–224, 393–400

Merchel, S., Arnold, M., Aumaitre, G., Benedetti, L., Bourlès, D.L., Braucher, R., Alfimov, V., Freeman, S.P.H.T., Steier, P., Wallner, A., 2008. Towards more precise ^{10}Be and ^{36}Cl data from measurements at the 10–14 level: influence of sample preparation. Nuclear Instruments and Methods in Physics Research B 266, 4921–4926.

Mifsud, C., Fujioka, T., Fink, D., 2013. Extraction and purification of quartz in rock using hot phosphoric acid for in situ cosmogenic exposure dating. Nucl. Instrum. Nuclear Instruments and Methods in Physics Research B 268, 1179-1184.

Schimmelpfennig, I., Benedetti, L., Finkel, R., Pik, R., Blard, P.H., Bourlès, D., Burnard, P., Williams, A., 2009. Sources of in-situ ^{36}Cl in basaltic rocks. Implications for calibration of production rates. Quaternary Geochronology. 4, 441-461.

Nishiizumi, K., Winterer, E.L., Kohl, C.P., Klein, J., Middleton, R., Lal, D., Arnold, J.R., 1989. Cosmic ray production rates of ^{10}Be and ^{26}Al in quartz from glacially polished rocks. Journal of Geophysical Research. 94, 9.

Putnam, A.E., Schaefer, J.M., Barrell, D.J.A., Vandergoes, M., Denton, G.H., Kaplan, M.R., Finkel, R.C., Schwartz, R., Goehring, B.M., Kelley, S.E., 2010. In situ cosmogenic ^{10}Be production-rate calibration from the Southern Alps, New Zealand. Quaternary Geochronology, 5, 392-409.

Sharma P., Kubik P. W., Fehn U., Gove H. E., Nishiizumi K., Elmore D., 1990,Development of ^{36}C1 standards for AMS. Nuclear Instruments and Methods in Physics Research B 52, 410-415.

Schimmelpfennig I., L. Benedetti, V. Garreta, R. Pik, P-Henri Blard, P. Burnard, D. Bourlès, R. Finkel, K. Ammon, T. Dunai, 2011. Calibration of cosmogenic ^{36}Cl production rates from Ca and K spallation in lava flows from Mt. Etna (38°N, Italy) and Payun Matru (36°S, Argentina), Geochimica et Cosmochimica Acta, 75, 10,2611-2632.

Stone, J.O., 2000. Air pressure and cosmogenic isotope production. Journal of Geophysical

Research, 105, 23753-23759.

Verstraete, J., 2005. Approche multi-technique et multi-échelle d'étude des propriétés structurales des matériaux hétérogènes : application à un granulat siliceux naturel. Ph. D. Thesis, Mulhouse Univ.

Zerathe S., Braucher R., Lebourg T., Bourlès D., Manetti M., Léanni L. 2013. Dating chert (diagenetic silica) using in-situ produced 10Be: Possible complications revealed through a comparison with ^{36}Cl applied to coexisting limestone . Quaternary Geochronology, Volume 17, 81-93.

Zerathe S., Blard P-H., Braucher R., Bourlès D., Audin L., Carcaillet J., Delgado F., Benavente C., 2017,Toward the feldspar alternative for cosmogenic ^{10}Be applications. Quaternary Geochronology, 41, 83-96.

Table 1: Sample identification (as named when sampled and simplified short identification).

Table 2: Presentation of the different cleaning steps. The names (Bulk, HF, KOH and KOH-*bis*) refer to cleaning sequences (see text); "Yes" in a cell means that the cleaning step indicated in the first column has been performed.

Table 3: Tables 3: Sample analytical data and cosmogenic nuclide concentrations. (1-KOH and 1 KOH-*bis* not prepared because of lack of sample)

Table 4 : Leaching efficiency; This "efficiency" represents, for a given cleaning step (HF, KOH) the mass dissolved divided by the volume of solution used; (In case of HF, the volume is the total volume used for the 3 sequential leachings)

Table 5: Denudation rates and minimum exposure ages for the studied samples.

Figure 1: Photography of Sample 1 (13-IL-ZEB-01). Limestone (light brown) has been used to determine the ^{36}Cl concentrations and the chert fraction (dark brown) for the determination of ^{10}Be and ^{26}Al concentrations.

Figure 2: Evolution of ^{10}Be concentrations as a function of the cleaning process steps.

Figure 3: Evolution of ^{27}Al concentration as a function of the cleaning process steps.

Figure1

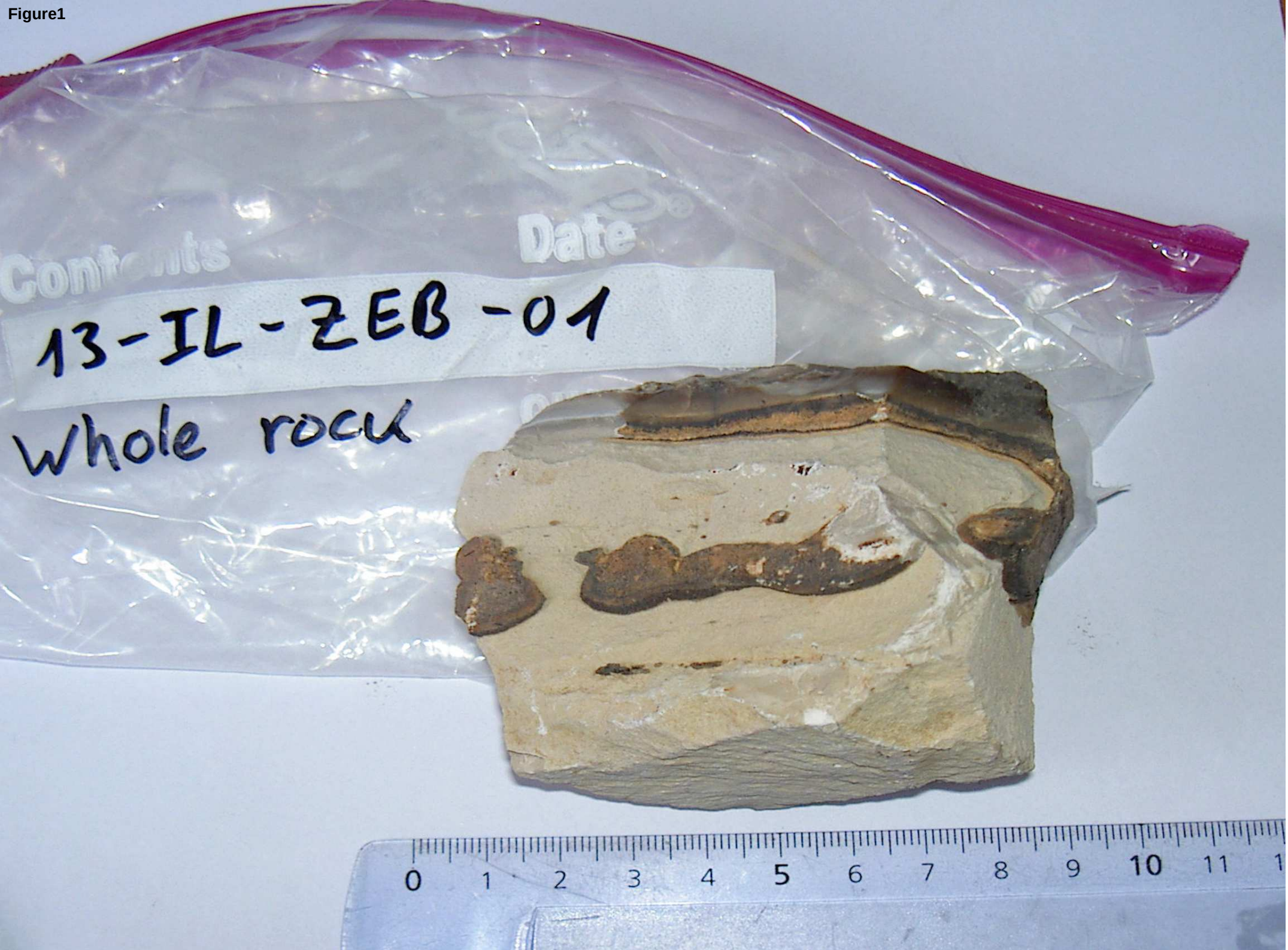

Figure2

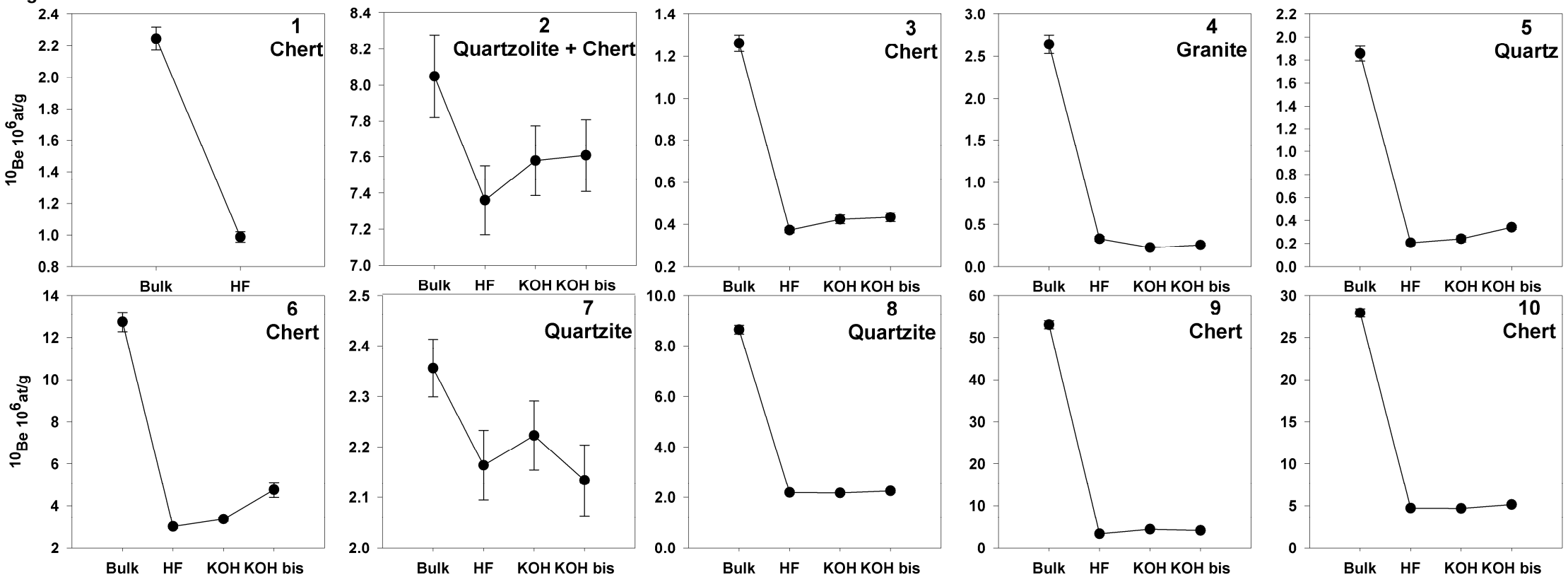
1
Chert
2
Quartzolite + Chert
3
Chert
4
Granite
5
Quartz
6
Chert
7
Quartzite
8
Quartzite
9
Chert
10
Chert
^{10}Be 10^{6}at/g
Bulk
HF
KOH
KOH bis

Figure3

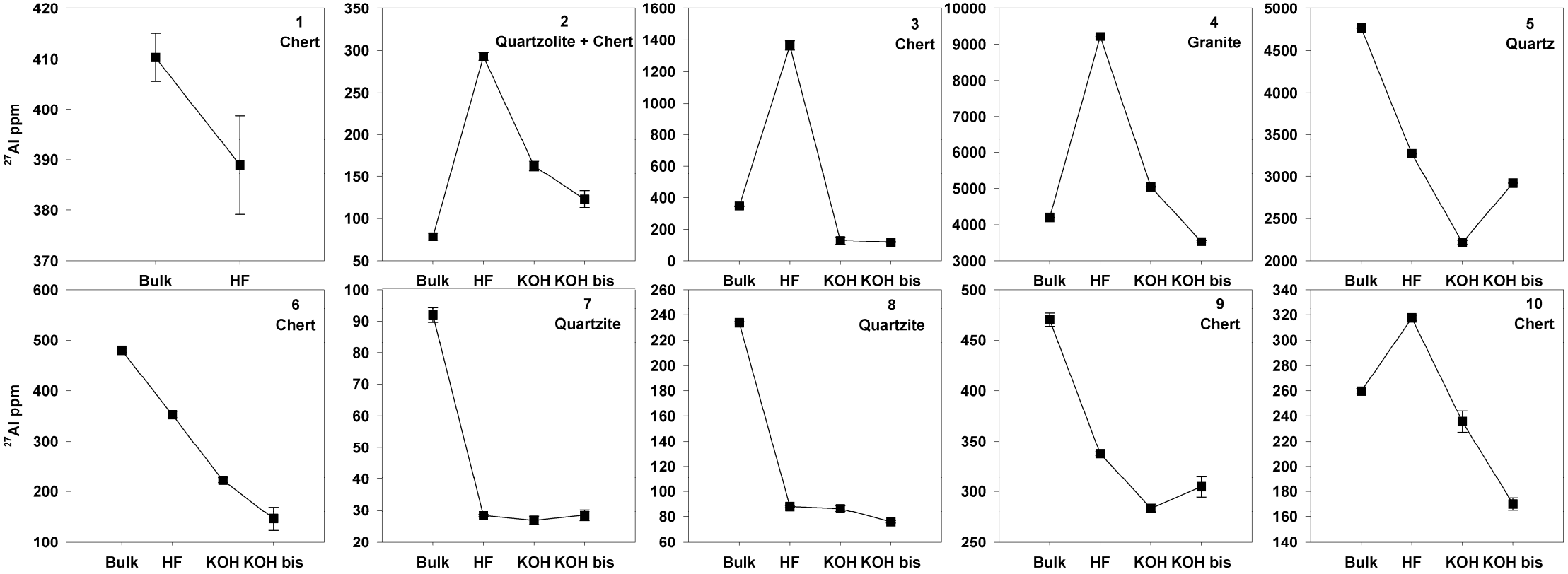
^{27}Al ppm
1
Chert
2
Quartzolite + Chert
3
Chert
4
Granite
5
Quartz
6
Chert
7
Quartzite
8
Quartzite
9
Chert
10
Chert
Bulk
HF
KOH
KOH bis

Table 1: Sample identification (as named when sampled and simplified short identification).

Sample ID	Short ID	Latitude	Longitude	Alt.(m)	Type
13-IL-ZEB-01	1	31.020	35.285	83	"Zebra surface" Limestone clast with chert inside; chert band from ~2 cm depth; coarse fraction
13-IL-ZEB-02	2	31.020	35.285	83	"Zebra surface" Quartzolite sample; at surface and homogeneous; coarse fraction
13-IL-YEH-09	3	29.561	34.892	357	"Wadi Yehoshafhat" fractured chert amalgam (50-60 clasts)
13-IL-YEH-10	4	29.561	34.892	359	"Wadi Yehoshafhat" fractured granite amalgam (~80 clasts)
13-IL-YEH-11	5	29.561	34.892	359	"Wadi Yehoshafhat" quartz vein in Precambrian granite bench
13-IL-ARAD-14	6	31.227	35.210	637	"Mount Kina" near Arad; ~40 clast chert amalgam from gently sloping pads near hill crest
13-IL-ARAD-15	7	31.227	35.210	637	"Mount Kina" near Arad; ~40 clast quartzalite amalgam from gently sloping pads near hill crest
13-IL-HEM-17	8	31.132	35.170	434	"Hemar Formation" desert pavement atop mesa; quartzalite pebble amalgam (40-50)
13-IL-HEM-18	9	31.132	35.170	434	"Hemar Formation" desert pavement atop mesa; Imported Chert* pebble amalgam (40-50)
13-IL-HEM-19	10	31.132	35.170	434	"Hemar Formation" desert pavement atop mesa; senonian chert** pebble amalgam (40-50)

* Imported chert: Eocene Chert transported from east of the Dead Sea rift to lts current location by Miocene drainage systems.

** Senonian chert : chert clasts derived from local bedrock outcrops

Table 2: Presentation of the different cleaning steps. The names (Bulk, HF, KOH and KOH-*bis*) refer to cleaning sequences (see text); "Yes" in a cell means that the cleaning step indicated in the first column has been performed.

Cleaning steps	**Sample**			
Crushing / Sieving (0.25-1mm)	**Yes**			
	Crushed sample divided in 4 sub samples			
	Sub-Sample - BULK	**Sub-Sample - HF**	**Sub-Sample - KOH**	**Sub-Sample - KOH-*bis***
Aqua regia		**Yes**	**Yes**	**Yes**
H_2SiF_6 -HCL		**Yes**	**Yes**	**Yes**
Meteoritic ^{10}Be removal (3sequential dissolutions in 48% HF		**Yes**	**Yes**	**Yes**
3N KOH / 80°C- 2 days			**Yes**	**Yes**
3N KOH / 80°C- 2 days				**Yes**
Total dissolution (10Ml HNO_3; 3Ml $HClO_4$	**Yes**	**Yes**	**Yes**	**Yes**
^{27}Al determination	**Yes**	**Yes**	**Yes**	**Yes**
AMS Measurements	**Yes**	**Yes**	**Yes**	**Yes**

Tables 3: Sample analytical data and cosmogenic nuclide concentrations. (1-KOH and 1 KOH-*bis* not prepared because of lack of sample)

Sample	Sub samples	Mass	^{10}Be	^{27}Al	^{26}Al
		g	Mat/g	ppm	Mat/g
13-IL-ZEB-01	1-Bulk	7.02	2.24 ± 0.07	410.3 ± 4.8	2.52 ± 0.24
	1-HF	3.03	0.99 ± 0.03	388.9 ± 9.8	n.a.
13-IL-ZEB-02	2-Bulk	18.31	8.05 ± 0.23	78.4 ± 4.8	2.54 ± 0.25
	2-HF	4.08	7.36 ± 0.19	293.1 ± 4.5	7.69 ± 2.06
	2-KOH	3.50	7.58 ± 0.19	162.6 ± 5.6	n.a.
	2-KOH-*bis*	3.00	7.61 ± 0.2	123.1 ± 10.1	9.17 ± 0.8
13-IL-YEH-09	3-Bulk	12.92	1.26 ± 0.04	346.6 ± 1.9	1.69 ± 0.1
	3-HF	5.70	0.37 ± 0.01	1364.1 ± 28.8	n.a.
	3-KOH	3.36	0.42 ± 0.02	127.9 ± 24.6	n.a.
	3-KOH-*bis*	3.38	0.43 ± 0.02	116.7 ± 2	n.a.
13-IL-YEH-10	4-Bulk	17.73	2.64 ± 0.11	4196 ± 1.2	0.11 ± 0.13
	4-HF	7.73	0.33 ± 0.03	9225 ± 1.9	5.29 ± 6.56
	4-KOH	7.05	0.23 ± 0.01	5048.9 ± 11	1.14 ± 1.19
	4-KOH-*bis*	6.39	0.26 ± 0.02	3533.2 ± 29.6	n.a. (^{26}Al/^{27}Al < blank)
13-IL-YEH-11	5-Bulk	17.33	1.86 ± 0.06	4768.7 ± 2.2	0.09 ± 0.11
	5-HF	11.55	0.21 ± 0.02	3269.4 ± 2.2	1.54 ± 0.72
	5-KOH	10.51	0.24 ± 0.03	2218.5 ± 25.7	0.41 ± 0.16
	5-KOH-*bis*	11.22	0.34 ± 0.02	2920.4 ± 0.9	0.38 ± 0.23
13-IL-ARAD-14	6-Bulk	16.59	12.74 ± 0.46	479.3 ± 3.8	9.05 ± 0.81
	6-HF	9.65	3.01 ± 0.09	352.5 ± 6.6	12.13 ± 0.96
	6-KOH	4.95	3.36 ± 0.11	221.6 ± 4.7	10.8 ± 0.65
	6-KOH-*bis*	2.86	4.75 ± 0.36	145.9 ± 23	n.a.
13-IL-ARAD-15	7-Bulk	16.46	2.36 ± 0.06	92 ± 2.4	n.a.
	7-HF	11.29	2.16 ± 0.07	28.3 ± 0.4	n.a.
	7-KOH	11.33	2.22 ± 0.07	26.8 ± 1.3	n.a.
	7-KOH-*bis*	10.59	2.13 ± 0.07	28.4 ± 1.8	0.3 ± 0.1
13-IL-HEM-17	8-Bulk	17.03	8.64 ± 0.17	233.7 ± 1	9.59 ± 0.61
	8-HF	11.23	2.19 ± 0.07	88.2 ± 0.8	n.a.
	8-KOH	11.14	2.16 ± 0.07	86.4 ± 2.3	9.63 ± 0.7
	8-KOH-*bis*	10.44	2.24 ± 0.07	75.9 ± 1	8.79 ± 1.05
13-IL-HEM-18	9-Bulk	14.59	52.99 ± 0.95	470.1 ± 6.3	6.28 ± 0.58
	9-HF	7.44	3.33 ± 0.11	337.6 ± 2	8.15 ± 0.41
	9-KOH	5.08	4.38 ± 0.15	283.3 ± 4.2	8.42 ± 0.53
	9-KOH-*bis*	1.90	4.1 ± 0.13	304.6 ± 10.2	8.7 ± 1.91
13-IL-HEM-19	10-Bulk	18.50	27.92 ± 0.49	259.6 ± 2.1	6.38 ± 0.45
	10-HF	11.67	4.71 ± 0.13	317.4 ± 2.2	11.41 ± 0.51
	10-KOH	4.86	4.68 ± 0.15	235.6 ± 8.3	9.64 ± 1.03
	10-KOH-*bis*	3.40	5.13 ± 0.16	170.1 ± 4.8	6.52 ± 1.26

Sample	Mass	^{36}Cl	^{35}Cl	Ca
	g	Mat/g	ppm	%
13-IL-ZEB-01	46.54	3.36±0.11	2.49 ± 0.08	37.4
13-IL-ZEB-02	17.59	7.30±0.25	2.49 ± 0.08	41.0

Table 4 : Leaching efficiency; This “efficiency” represents, for a given cleaning step (HF, KOH) the total mass dissolved divided by the volume of solution used; (In case of HF, the volume is the sum of the three HF volumes used to perform the three sequential leachings)

Short ID	Sample type	Leaching efficiency (g/ml)		
		HF	KOH	KOH-*bis*
1-HF	Chert within carbonate matrix	0.51	-	-
2-HF	Quartzolite/dispersed chert and carbonate	0.65	-	-
2-KOH		0.59	0.05	-
2-KOH-*bis*		0.75	0.02	0.001
3-HF	Amalgamated pebbles (chert)	0.52	-	-
3-KOH		0.55	0.08	-
3-KOH-*bis*		0.55	0.07	0.075
4-HF	Amalgamated pebbles (granite)	0.52	-	-
4-KOH		0.54	0.01	-
4-KOH-*bis*		0.51	0.04	0.004
5-HF	Amalgamated pebbles (quartz vein)	0.32	-	-
5-KOH		0.32	0.05	-
5-KOH-*bis*		0.29	0.06	0.003
6-HF	Amalgamated pebbles (chert)	0.38	-	-
6-KOH		0.42	0.22	-
6-KOH-*bis*		0.42	0.17	0.087
7-HF	Amalgamated pebbles (quartzite)	0.29	-	-
7-KOH		0.28	0.01	-
7-KOH-*bis*		0.28	0.01	0.005
8-HF	Amalgamated pebbles (quartzite)	0.29	-	-
8-KOH		0.28	0.03	-
8-KOH-*bis*		0.30	0.01	0.004
9-HF	Amalgamated pebbles (chert)	0.46	-	-
9-KOH		0.38	0.17	-
9-KOH-*bis*		0.39	0.16	0.103
10-HF	Amalgamated pebbles (chert)	0.34	-	-
10-KOH		0.51	0.16	-
10-KOH-*bis*		0.36	0.26	0.112

Table 5: Denudation rates and minimum exposure ages for the studied samples.

	Location name	^{10}Be		^{36}Cl	
		Denudation rates	Exposure ages	Denudation rates	Exposure ages
Short ID		m/Ma	ka	m/Ma	ka
1-Bulk	ZEB	0.72 ± 0.02	638 ± 69	2.19 ± 0.07	275 ± 9
1-HF		2.15 ± 0.07	256 ± 25		
2-Bulk		n.a.	Saturated	0.18 ± 0.01	1065 ± 37
2-HF		0	Saturated		
2-KOH		0	Saturated		
2-KOH-*bis*		0	Saturated		
3-Bulk	YEH	2.08 ± 0.06	267 ± 26		
3-HF		8.41 ± 0.3	75 ± 7		
3-KOH		7.3 ± 0.35	86 ± 9		
3- KOH-*bis*		7.11 ± 0.35	88 ± 9		
4-Bulk		0.79 ± 0.03	606 ± 67		
4-HF		9.66 ± 0.82	66 ± 8		
4-KOH		14.59 ± 0.8	45 ± 5		
4-KOH bis		12.75 ± 1.08	51 ± 6		
5-Bulk		1.28 ± 0.04	406 ± 42		
5-HF		16.01 ± 1.28	41 ± 5		
5-KOH		13.55 ± 1.53	48 ± 7		
5- KOH-*bis*		9.31 ± 0.5	69 ± 7		
6-Bulk	ARAD	n.a.	Saturated		
6-HF		0.92 ± 0.03	536 ± 56		
6-KOH		0.79 ± 0.02	610 ± 65		
6- KOH-*bis*		0.46 ± 0.03	927 ± 134		
7-Bulk		1.28 ± 0.03	407 ± 40		
7-HF		1.42 ± 0.05	371 ± 37		
7-KOH		1.38 ± 0.04	382 ± 38		
7- KOH-*bis*		1.45 ± 0.05	365 ± 37		
8-Bulk	HEM	0.04 ± 0.00	3090 ± 646		
8-HF		1.15 ± 0.04	444 ± 45		
8-KOH		1.17 ± 0.04	439 ± 45		
8- KOH-*bis*		1.11 ± 0.04	457 ± 47		
9-Bulk		n.a.	Saturated		
9-HF		0.63 ± 0.02	722 ± 79		
9-KOH		0.4 ± 0.01	1018 ± 122		
9- KOH-*bis*		0.45 ± 0.01	935 ± 108		
10-Bulk		n.a.	Saturated		
10-HF		0.35 ± 0.01	1119 ± 134		
10-KOH		0.35 ± 0.01	1111 ± 135		
10- KOH-*bis*		0.29 ± 0.01	1259 ± 159		